ACCOUNTS of chemical research

Article

pubs.acs.org/accounts

Organic Electronic Materials: Recent Advances in the DFT Description of the Ground and Excited States Using Tuned Range-Separated Hybrid Functionals

Thomas Körzdörfer*[,†] and Jean-Luc Brédas*[,‡,§]

[†]Computational Chemistry, Institute of Chemistry, University of Potsdam, D-14476 Potsdam, Germany

[‡]School of Chemistry and Biochemistry and Center for Organic Photonics and Electronics, Georgia Institute of Technology, Atlanta, Georgia 30332, United States

CONSPECTUS: Density functional theory (DFT) and its time-dependent extension (TD-DFT) are powerful tools enabling the theoretical prediction of the ground- and excited-state properties of organic electronic materials with reasonable accuracy at affordable computational costs. Due to their excellent accuracy-to-numerical-costs ratio, semilocal and global hybrid functionals such as B3LYP have become the workhorse for geometry optimizations and the prediction of vibrational spectra in modern theoretical organic chemistry. Despite the overwhelming success of these out-of-the-box functionals for such applications, the computational treatment of electronic and structural properties that are of particular interest in organic electronic materials sometimes reveals severe and qualitative failures of such functionals. Important examples include the overestimation of conjugation, torsional barriers, and electronic coupling as well as the underestimation of bond-length alternations or excited-state energies in low-band-gap polymers.

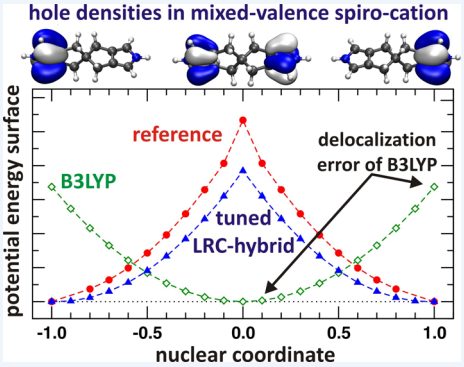

In this Account, we highlight how these failures can be traced back to the delocalization error inherent to semilocal and global hybrid functionals, which leads to the spurious delocalization of electron densities and an overestimation of conjugation. The delocalization error for systems and functionals of interest can be quantified by allowing for fractional occupation of the highest occupied molecular orbital. It can be minimized by using long-range corrected hybrid functionals and a nonempirical tuning procedure for the range-separation parameter.

We then review the benefits and drawbacks of using tuned long-range corrected hybrid functionals for the description of the ground and excited states of π-conjugated systems. In particular, we show that this approach provides for robust and efficient means of characterizing the electronic couplings in organic mixed-valence systems, for the calculation of accurate torsional barriers at the polymer limit, and for the reliable prediction of the optical absorption spectrum of low-band-gap polymers. We also explain why the use of standard, out-of-the-box range-separation parameters is not recommended for the DFT and/or TD-DFT description of the ground and excited states of extended, pi-conjugated systems. Finally, we highlight a severe drawback of tuned range-separated hybrid functionals by discussing the example of the calculation of bond-length alternation in polyacetylene, which leads us to point out the challenges for future developments in this field.

INTRODUCTION

Over the past decade, organic electronic materials have made their way from the research laboratories all over the globe to the everyday life of millions of users worldwide. In particular, the success of organic light-emitting diodes, which steadily replace their inorganic competition in small (smart phones) and medium-sized (tablets) displays, paves the way for the further development of new and improved organic electronic materials and devices. Ever since the discovery of conducting polymers almost 40 years ago,[1] the developments in this field of research have benefitted from a strong input from theory. Computer-based electronic-structure calculations provide important insights into the electronic properties of organic electronic materials, elucidate the basic physical principles that underlie charge and exciton transport, substantiate experimental results, and assist in the design of novel materials. While the field has been dominated by the use of semiempirical model Hamiltonians for many years, density functional theory (DFT) has become today the most commonly used electronic-structure method for the description of the ground and excited states of organic electronic materials.[2,3]

Due to its excellent accuracy-to-computational costs ratio, DFT lends itself as the natural choice for the theoretical description of the electronic structure of organic electronic materials. With modern computer architectures, systems containing thousands of electrons can be readily evaluated when using the most effective DFT functionals. DFT generally

Special Issue: DFT Elucidation of Materials Properties

Received: January 16, 2014
Published: April 30, 2014

predicts the ground-state geometries, vibrational spectra, and electron−phonon couplings in most organic molecules with high accuracy and yields a qualitatively and often also quantitatively correct picture of the electronic structure of molecules, crystals, metallic systems, and metal−organic interfaces. The time-dependent extension of DFT (TDDFT)[4] allows the calculation and interpretation of optical absorption and emission spectra and assists in studying exciton transfer and charge-recombination processes in organic electronic devices.

While DFT has become an invaluable tool for studying a variety of electronic and structural properties of organic electronic materials, improving the accuracy and efficiency of DFT calculations remains a major challenge for the electronic-structure community. Both the accuracy and computational costs of DFT are vastly determined by the choice for the approximate exchange-correlation (xc) functional $E_{xc}[n]$, or its density functional derivative, the xc potential $v_{xc}[n](\mathbf{r}) = dE_{xc}[n]/dn(\mathbf{r})$. Many different approximations to $E_{xc}[n]$ exist in the literature, some of them solely based on physical principles, some of them highly empirical. Commonly used approaches are the so-called semilocal approximations, which include the local-density approximation (LDA),[3] generalized-gradient approximations (GGAs) such as the functional of Perdew, Burke, and Ernzerhof (PBE),[5] and meta-GGAs such as M06L.[6] While semilocal functionals can be very useful, global hybrid functionals that include a fixed, global fraction of explicit Hartree−Fock (HF) exchange such as B3LYP[7] (20%), the PBE-hybrid PBEh[8] (25%, also known as PBE0 or PBE1PBE), or M06[9] (27%) are considered today as the typical workhorses for theoretical organic chemistry. This is because the (partial) inclusion of explicit HF exchange yields overall an improved description of many molecular properties, such as geometries, binding energies, vibrational frequencies, excitation energies, and more.

Despite the success of B3LYP and other global hybrids that include 20−30% HF exchange, these functionals also show some severe and qualitative failures for several properties of interest in organic electronic materials research. In fact, many of these deficiencies are related, in one way or another, to what can be described as the many-electron self-interaction error (MSIE)[10,11] or the localization/delocalization error. In this Account, we highlight how this error influences the DFT description of the ground and excited states of organic electronic materials and the way it can be quantified. We then discuss our recent efforts to reduce the localization/delocalization error in the description of organic materials by using range-separated hybrid functionals that have the correct asymptotic behavior and system-specific range-separation parameters that are tuned to minimize the localization/delocalization error. We start our discussion by demonstrating the consequences of the localization/delocalization error for a simple model system.

THE LOCALIZATION/DELOCALIZATION ERROR

The model system we choose to introduce the localization/delocalization error is He_3^+, where the He atoms are aligned linearly and the interatomic distance R between the He atoms is varied between 1 and 7 Å. Figure 1 shows the Mulliken charge on the central He atom as a function of R calculated with several electronic-structure methods. We note that, by considering three He atoms, we allow single-reference methods to localize the charge at the central He without the need to break symmetry. A full configuration interaction (FCI) calculation,[12] which we consider as the reference here, localizes the positive charge on the central He for large interatomic distances. In contrast, all

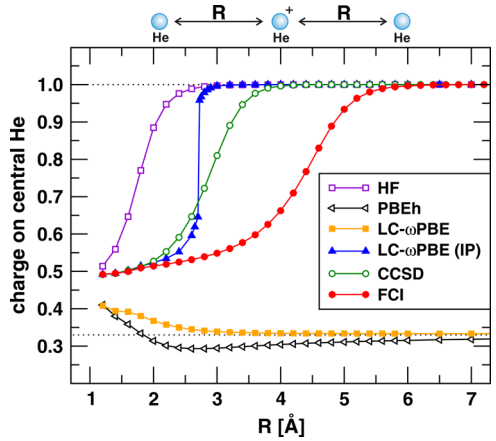

Figure 1. Mulliken charge on central He atom in He_3^+ as a function of the interatomic distance R calculated from HF, PBEh, standard ($\omega = 0.4$ bohr^{-1}), and IP-tuned LC-ωPBE, CCSD, and full CI (FCI).

standard DFT functionals such as LDA, GGAs, and standard global hybrid functionals spuriously delocalize the charge over all three He atoms, even for large R values. In Figure 1, this is exemplified by the PBEh curve, which is representative of all semilocal and standard global hybrid functionals. Importantly, the delocalization error not only occurs at large interatomic distances, but for all values of R. This can be explained by the observation that semilocal exchange functionals, in contrast to full exact exchange, do not cancel the spurious Coulombic self-interaction, leading to a self-repulsion of localized one-electron densities.[13] Consequently, the delocalization error is often also referred to as self-interaction error.[10,11]

In contrast to standard DFT functionals, Hartree−Fock (HF) and coupled-cluster singles-doubles (CCSD) localize the charge on the central He atom; however, the localization occurs at much smaller distances as compared to the FCI reference. We refer to this error of the HF approach as the localization error. As with every error of HF theory, the localization error is a consequence of missing correlation. In fact, a significant part of the localization error is made up by the missing static correlation, that is, by the incapacity to mix the three configurations in which the charge is localized on either one of the three He atoms. The importance of static correlation is also reflected by the poor performance of the CCSD approach, which is unable to apprehend the multi-reference character of the He_3^+ ground state at large R. Due to the close relation of the delocalization error to the missing static correlation, the localization error has also been referred to as the static correlation error.[14]

In the literature, the localization/delocalization error is frequently discussed in the context of fractional particle numbers, which can be introduced into the DFT formalism by coupling the system to a bath of particles.[15] The implications of this concept have been discussed in several review articles;[16−18] thus, we only provide a brief summary here. As demonstrated in the seminal paper of Perdew and co-workers,[15] the exact total energy as a function of fractional particle number is a series of straight lines with kinks at integer occupations. The slope of these straight lines corresponds to the respective HOMO eigenvalues. Both HF and standard DFT functionals fail to reproduce this straight-line condition. The typical failures are schematically illustrated in Figure 2. HF theory favors integer particle numbers over fractional ones, which explains why HF tends to localize the electron density. In contrast, standard DFT functionals give too

dx.doi.org/10.1021/ar500021t | Acc. Chem. Res. 2014, 47, 3284−3291

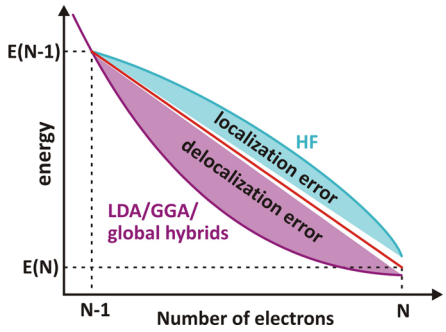

Figure 2. Schematic representation of the localization error of HF theory and the delocalization error in standard DFT functionals. Despite good agreement with the exact values (red curve) at the integer points, the convex [concave] behavior of DFT [HF] leads to a lower [higher] energy for fractional charges.

low energies for fractional particle numbers, which explains why these functionals spuriously favor delocalized electron densities. One way to quantify the (de)localization error of HF and standard DFT functionals is to calculate the deviation of the energy curve from the expected linearity,[19] which is expressed as

$$\Delta E(N+\delta) = E(N+\delta) - E(N) - [E(N+1) - E(N)]\delta \quad (1)$$

where N is an integer and $0 \leq \delta \leq 1$. ΔE vanishes for integer particle numbers. For fractional particle numbers, however, ΔE only vanishes if $E(N+\delta)$ is linear in δ, as is the case for the exact functional. A positive integral over $\int_0^1 \Delta E(N+\delta)\, d\delta$ is referred to as a localization error, while a negative integral is referred to as a delocalization error (see shaded areas in Figure 2). The localization/delocalization error is directly related to several notorious failures of semilocal and global hybrid functionals in the prediction of the ground and excited states of organic electronic materials, as will be highlighted below.

LONG-RANGE CORRECTED HYBRID FUNCTIONALS

One of the major issues of global hybrid functionals with a fixed fraction of HF exchange is to find a good trade-off between semilocal and HF exchange. One the one hand, full HF exchange is needed for a complete correction of self-interaction and, thus, a correct description of the asymptotic region of the xc potential. On the other hand, however, semilocal exchange is known to mimic short-range static correlation effects that are important for chemical bonding. While global hybrids have to choose between semilocal and HF exchange, the concept of range-separated hybrid functionals facilitates the combination of the best of these both worlds.[20] The central premise underlying these functionals is the partitioning of the Coulomb-Operator into short-range (SR) and long-range (LR) components, which is typically achieved with the help of the standard error function (erf):

$$\frac{1}{r_{12}} = \frac{\mathrm{erf}(\omega r_{12})}{r_{12}} + \frac{1 - \mathrm{erf}(\omega r_{12})}{r_{12}} \quad (2)$$

The error function varies smoothly from $\mathrm{erf}(0) = 0$ to $\mathrm{erf}(\infty) = 1$. The range-separation is determined by the parameter ω, where $1/\omega$ defines a characteristic length scale for the transition between the SR and LR descriptions. By treating SR and LR electron−electron interactions on a different footing, the range-separation scheme allows one to incorporate semilocal or standard hybrid DFT within the SR part of the Coulomb operator and full HF exchange plus semilocal correlation in the LR component. This particular class of range-separated hybrids is referred to as long-range corrected (LRC) hybrid functionals. LRC hybrids restore the correct $1/r$-asymptotic tail of the exchange-correlation potential (hence the term long-range corrected), thereby improving the description of several molecular properties that are sensitive to LR interactions. Here, results from the LRC-hybrids LC-ωPBE[21] and ωB97[22] will be reviewed.

A main message of this Account is that LRC hybrid functionals represent a most valuable approach for the (approximate) minimization of the localization/delocalization error described above.[18] This can be understood by the fact that, in contrast to HF and semilocal DFT functionals, LRC hybrid functionals allow the combination of a full correction of self-interaction in the LR with the treatment of static correlation effects (mimicked by the semilocal exchange functional) in the SR. Hence, these functionals facilitate the reduction of both the self-interaction error and the static correlation error in a single instance. In other words, by treating LR interactions with (localizing) full HF exchange and SR interactions by (delocalizing) semilocal DFT, LRC hybrids intrinsically counteract both the spurious localization error of HF and the spurious delocalization error of semilocal DFT. As a consequence, the degree of electronic (de)localization in LRC hybrids is primarily determined by the length scale of the range-separation, that is, the inverse range-separation parameter $1/\omega$.

IP-TUNING PROCEDURE FOR π-CONJUGATED MOLECULAR CHAINS

Ever since the inception of the range-separated hybrid functionals,[20] it has been argued that ω should be a functional of the electron density. However, the exact density dependence of ω is not known. Consequently, most range-separated hybrid functionals employ a fixed, empirical value for ω.[21,22] To allow for a more flexible range-separation, a frequently employed strategy is to determine the optimal range-separation parameter for each system *separately* by enforcing the functional to obey known properties of the exact functional. In this context, the range-separation parameter is often determined by minimizing the difference between the highest occupied molecular orbital (HOMO) eigenvalue and the computed ionization potential (IP):

$$\Delta_{\mathrm{IP}}(\omega) = |-\varepsilon^{\omega}_{\mathrm{HOMO}} - (E_{\mathrm{gs}}(\omega, N) - E_{\mathrm{gs}}(\omega, N-1))| \quad (3)$$

This IP-tuning procedure[23] has been shown to improve the description of properties related to the IP and the fundamental gap for a range of systems. The tuning is nonempirical, since it requires the approximate functional to obey a property that would be satisfied by the exact functional. In fact, this and similar tuning procedures have been applied to predict highly accurate IPs and band gaps;[18,24,25] the extension of this approach to predict full valence photoelectron spectra has also been discussed.[19,26] Here, however, we would like to point out an alternative interpretation of the IP-tuning procedure.

In fact, the IP-tuning can be interpreted as a minimization of the delocalization error at the level of the HOMO.[18] As the HOMO eigenvalue equals the slope of the total-energy evolution with δ, IP tuning guarantees that the initial slope of the total-energy curve at $\delta = 0^-$ (i.e., when going from the neutral to the cation state) equals the vertical IP (the total energy difference between the neutral and cation states). This, however, does not apply for the whole fractional-particle curve, which is why a

dx.doi.org/10.1021/ar500021t | Acc. Chem. Res. 2014, 47, 3284−3291

(typically very small) deviation from linearity can remain after IP tuning. Still, the localization/delocalization error at the HOMO level is significantly reduced in the IP-tuned LRC hybrids compared to HF and all commonly used semilocal, global hybrid, and standard LRC-hybrid functionals. This is highlighted in Figure 3, which shows the deviation from linearity $\Delta E(N+\delta)$ of

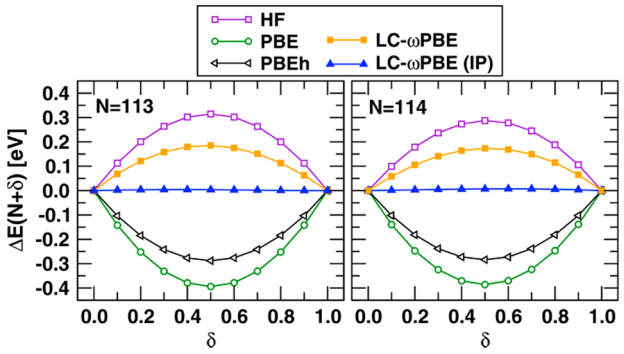

Figure 3. Deviation of the total energy from straight line (see eq 1) as a function of fractional-particle number δ for $C_{16}H_{18}$ (114 electrons) when inserting one electron into the HOMO (left) and LUMO (right) using HF, PBE, PBEh, as well as the standard (ω = 0.4 bohr^{-1}) and IP-tuned (see eq 3) LC-ωPBE functionals.

the total energy (see eq 1) as a function of the fractional particle number δ for the linear polyene $C_{16}H_{18}$ when inserting an electron into the HOMO and LUMO (lowest unoccupied molecular orbital). While HF and LC-ωPBE (using the standard ω-value of 0.4 bohr^{-1}) suffer from a significant localization error, the semilocal functional PBE and the global hybrid PBEh demonstrate a large delocalization error.

In LRC-hybrids with no (or a fixed amount of) HF exchange in the short-range, the (de)localization error is determined by the value of the range-separation parameter ω. In the case of the linear polyene $C_{16}H_{18}$, the standard ω of LC-ωPBE (ω = 0.4 bohr^{-1}) is found to be too large, thus leading to a large localization error. Application of the IP-tuning procedure drastically reduces the localization error in LC-ωPBE and an almost perfect straight-line behavior of the total energy curve between the cation and anion is found (see Figure 3). These results are exemplary for what is generally found for extended π-conjugated systems.[27]

It is important to keep in mind that a vanishing localization/delocalization error is a necessary, but not sufficient criterion for accurately describing the (de)localization of charges. Hence, the reduction of the localization/delocalization error in LRC hybrids typically only reduces, but not fully solves all problems related to charge (de)localization. As demonstrated in Figure 1, this is particularly true for situations in which the LR static correlation is dominant: While the IP-tuned LC-ωPBE curve correctly localizes the excess charge and significantly improves upon the HF result, the localization occurs very abruptly and at too short distances R. This can be ascribed to the fact that LRC hybrids only model the static correlation in the SR but not the LR.

It has been demonstrated that the IP-tuned ω value can vary significantly with system size.[24,25,27] Figure 4 shows the characteristic length $1/\omega$ obtained from IP-tuned LC-ωPBE as a function of the number of repeat units in four different molecular chains, that is, polyenes, alkanes, oligoacenes, and oligothiophenes. In all instances, the range-separation parameter decreases significantly with chain length. All IP-tuned ω values are smaller than the standard value ω = 0.4 bohr^{-1}. The

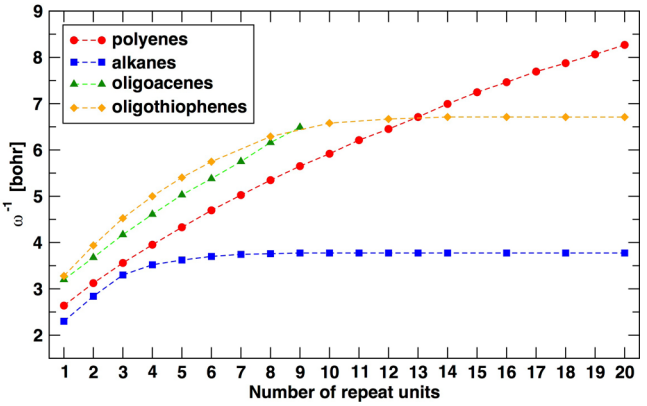

Figure 4. IP-tuned SR/LR separation parameters ($1/\omega$) in units of Bohr for linear polyene chains $C_{2n}H_{2n+2}$, alkane chains $C_{2n}H_{4n+4}$, oligoacenes, and oligothiophenes, as a function of the number of repeat units n.[27]

difference between the standard and IP-tuned ω values is particularly severe for chains with a very high degree of π-conjugation such as the polyenes and oligoacenes, for which the characteristic length $1/\omega$ increases almost linearly with the number of repeat units. For the alkane chains, however, the $1/\omega$ value saturates quickly; also their IP-tuned ω values are much closer to the standard ω value. This clearly demonstrates that not only the size but also the extent of conjugation plays an important role in determining the optimal ω values for a specific system of interest. A similar picture is seen for other LRC hybrids, independently of the form of the underlying semilocal functionals and the amount of HF exchange used in the SR.[27] Thus, generally speaking, the standard ω-values in LRC hybrids are not suitable for a reliable description of π-conjugated materials.

GROUND-STATE PROPERTIES

Organic Mixed-Valence Systems

Mixed-valence (MV) systems, which contain two or more redox centers in different oxidation states, are prototype systems that illustrate the major issues that can arise from the localization/delocalization error of HF and standard DFT functionals. The optical and electronic properties of MV systems are dominated by the interplay between the electronic coupling among redox centers and the reorganization energy.[28] Typically, highly correlated wave function methods are needed to capture the details of this competition, illustrating the importance of correlation effects. However, as many of the organic MV systems are too large to be treated with these methods, an important goal is to find a reliable description of MV systems at the cost of a HF or DFT calculation.

Due to their intrinsic localization/delocalization error, pure HF and standard DFT functionals are doomed to fail for such systems. This is illustrated by taking the example of the spiro-molecule shown in Figure 5a, a frequently studied prototypical organic MV system.[29] High-level post-HF methods have pointed out that the lower potential energy surface of this spiro-cation corresponds to a double well.[30] In contrast, semilocal and standard hybrid functionals symmetrically delocalize the excess charge over both redox centers (see Figure 5b). This spurious delocalization of the hole density is in line with the significant delocalization error (−0.26 eV) that is found when taking an electron out of the HOMO of the spiro-molecule. HF leads to the charge being localized on one of the redox centers (see Figure

dx.doi.org/10.1021/ar500021t | Acc. Chem. Res. 2014, 47, 3284−3291

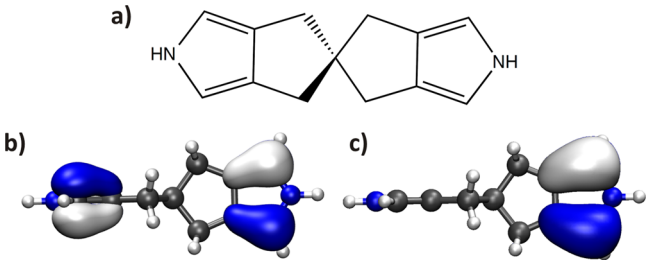

Figure 5. (a) Chemical structure of the spiro-molecule 5-methyl-5-((4-methyl-1*H*-pyrrol-3-yl)methyl)-2,4,5,6-tetrahydrocyclopenta[c]-pyrrole. (b) LUMO of the spiro-cation as predicted from B3LYP. (c) LUMO of the spiro-cation as predicted from HF.

5c) and, thus, to an electronic structure and geometry that are qualitatively consistent with the results of highly correlated post-HF methods. However, HF yields a significant localization error of +0.23 eV, which underlines that HF provides a correct description (and Robin-Day classification) for the wrong reason.

LRC-hybrid functionals can predict both the symmetric and symmetry-broken geometries, depending on the value chosen for the range-separation parameter ω.[29] Application of the IP-tuning procedure to a LRC-hybrid (here, ωB97) leads to a correct symmetry-broken geometry. To establish consistency between the geometries and the IP-tuned ω-values, the geometry relaxation and the IP-tuning procedure need to be iterated to self-consistency, which is typically the case after one to two geometry optimizations. As a consequence of this procedure, the localization error is reduced by several orders of magnitude. The corresponding potential energy surface corresponds to a double well, following closely the highly accurate equation-of-motion IP CCSD calculated ground-state energies (see Figure 6). This and other examples[29] validate the reliability of the IP-tuned LRC-hybrid approach for MV systems both qualitatively and quantitatively.

Torsion Potential Barrier in Polyenes

Another example where the delocalization error of standard DFT functionals becomes prominent is related to the torsional flexibility of π-conjugated molecular and polymer chains. This flexibility is typically severely underestimated by semilocal and global hybrid functionals,[31] which is a direct consequence of the

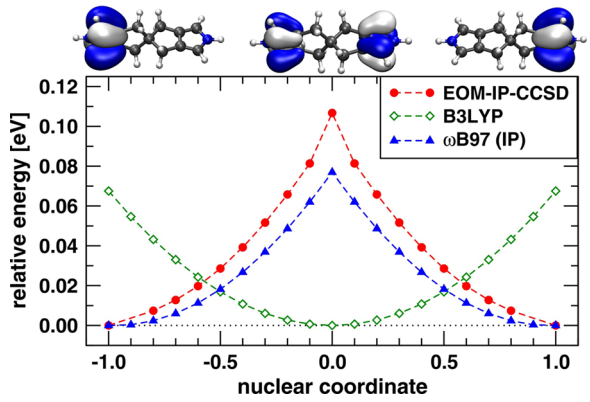

Figure 6. Potential energy surface for the spiro-cation as a function of the nuclear coordinate that connects the two symmetry-broken geometries ($\pm$1), as calculated with IP-tuned ωB97 (ω = 0.262 bohr^{-1}).[29] EOM-IP-CCSD and B3LYP results are given for comparison. Isosurface plots show the ωB97 hole density for the two symmetry-broken and the symmetric geometries.

delocalization error that overly stabilizes coplanar, fully conjugated conformations.[32]

The number of electronic structure methods that can be applied effectively to long molecular chains and, at the same time, are known to yield reliable results for torsional barriers remains very limited. Recently, it was demonstrated that dual-basis density-fitting MP2 (DB-DFMP2) provides for a good trade-off between accuracy and computational cost, allowing the application to long oligomers of polyacetylene.[31] Using the effective conjugation length (ECL) model introduced by Meier and co-workers,[33] the DB-DFMP2 calculated torsion barriers for oligomers of various lengths can be extrapolated to the polymer limit.

Figure 7 displays the evolution of the computed torsional barriers of the central C−C bond in linear polyene chains

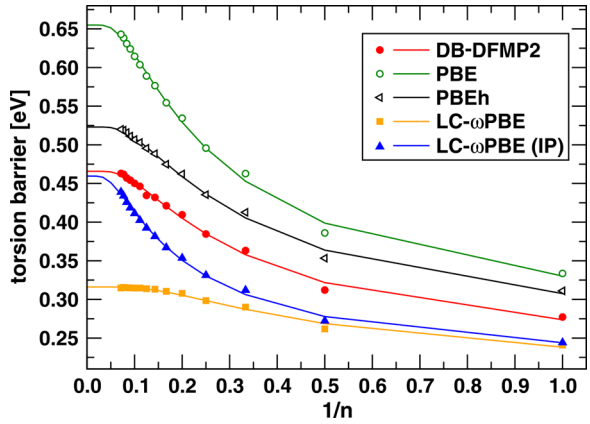

Figure 7. Evolution of the computed torsional barriers in polyacetylene for PBE, PBEh, standard (ω = 0.4 bohr^{-1}), and IP-tuned LC-ωPBE as a function of the inverse number of repeat units n compared to the DB-DFMP2 reference. The results for the torsion barriers are fitted using the effective conjugation length model[33] and extrapolated to the polymer limit (solid lines).[32]

$C_{2n}H_{2n+2}$ as a function of the inverse number of repeat units $1/n$ for various DFT functionals and DB-DFMP2, extrapolated to the polymer limit using the ECL-model (solid lines). As compared to the DB-DFMP2 reference, the semilocal PBE and the standard hybrid PBEh yield too large torsional barriers at the polymer limit. This is consistent with the large delocalization error found for these functionals, as exemplified in Figure 3. In contrast, standard LC-ωPBE (ω = 0.4 bohr^{-1}) yields a significant localization error, which is consistent with the severe underestimation of the torsional barrier. When this localization error is made to nearly vanish by using the IP-tuning procedure for each chain length, the evolution of the torsional barriers improves significantly and leads to a torsion barrier for polyacetylene in much better agreement with the DB-DFMP2 reference. In a recent study,[32] a similar picture was found not only for polyacetylene but also for polydiacetylene in the case of several other LRC-hybrids; thus, the choice of a suitable range-separation parameter is, in fact, a decisive factor in the performance of LRC-hybrids for the prediction of accurate torsion barriers in π-conjugated chains.

Bond-Length Alternation in Polyacetylene

The encouraging results for the torsional barriers in polyacetylene suggest that IP-tuned LRC-hybrids could also be a valuable approach to another notorious problem of electronic-structure methods, i.e., a reliable prediction of the degree of

dx.doi.org/10.1021/ar500021t | Acc. Chem. Res. 2014, 47, 3284−3291

bond-length alternation (BLA) representing the difference between the lengths of single-like and double-like bonds in π-conjugated chains. Due to their intrinsic delocalization error, standard semilocal and hybrid DFT functionals, which chemists extensively use for geometry optimizations, overestimate conjugation and hence typically underestimate the BLA significantly. This is illustrated in Figure 8, which compares the central BLA in linear polyenes obtained from PBE and PBEh to benchmark geometries obtained from CCSD(T). As compared to the experimental estimate of 0.08 Å,[35] extrapolation of the PBE and PBEh results to the polymer limit considerably underestimates the BLA in polyacetylene. When using the standard LC-ωPBE functional or pure HF exchange, the BLA converges much faster with the number of repeat units than in the CCSD(T) reference, leading to a significant overestimation of the BLA for all chain lengths. In the light of the localization/delocalization errors of the various functionals depicted in Figure 3, these findings do not come as a surprise.

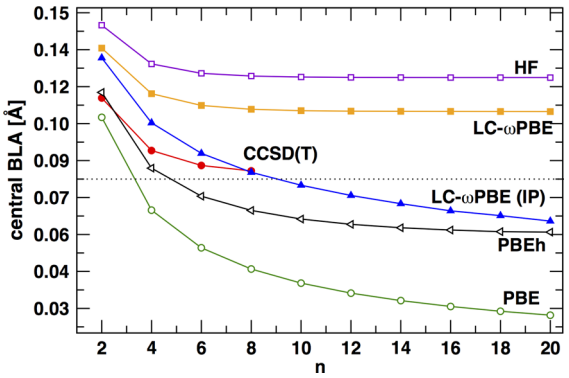

Figure 8. Central bond-length alternation (BLA) in polyenes H-(HC═CH)$_n$-H evaluated with various electronic-structure methods, as a function of the number of repeat units n.[34] The dotted line indicates the experimental estimate for the BLA in the polymer limit, 0.08 Å. CCSD(T) results serve as a reference for the short oligomers.

Application of the IP-tuning procedure, however, does not result in the anticipated behavior of the BLA. While the BLAs obtained from CCSD(T) saturate at around n = 8, the BLAs calculated from IP-tuned LRC hybrids do not show any sign of saturation up to n = 20, thus restoring one of the most obvious failures of the semilocal and global hybrid functionals.

A natural explanation for the failure of IP-tuned LC-ωPBE is provided by the evolution of the IP-tuned range-separation parameter with the number of repeat units depicted in Figure 4. The IP-tuned ω, and with it the BLA, decreases monotonically with increasing chain length in highly conjugated systems. By modifying ω with system size, we are changing the functional and, as a result, the effective Hamiltonian. Consequently, the IP-tuned LC-ωPBE approaches the semilocal PBE functional in the limit of long chains and an important property of standard LRC hybrids is lost, that is, size consistency. In fact, the lack of size consistency turns out to be the major drawback of tuned range-separated hybrid functionals.[34,36] Clearly, more work is needed to find approximations that allow reducing the localization/delocalization error without affecting the size-consistency of the method.

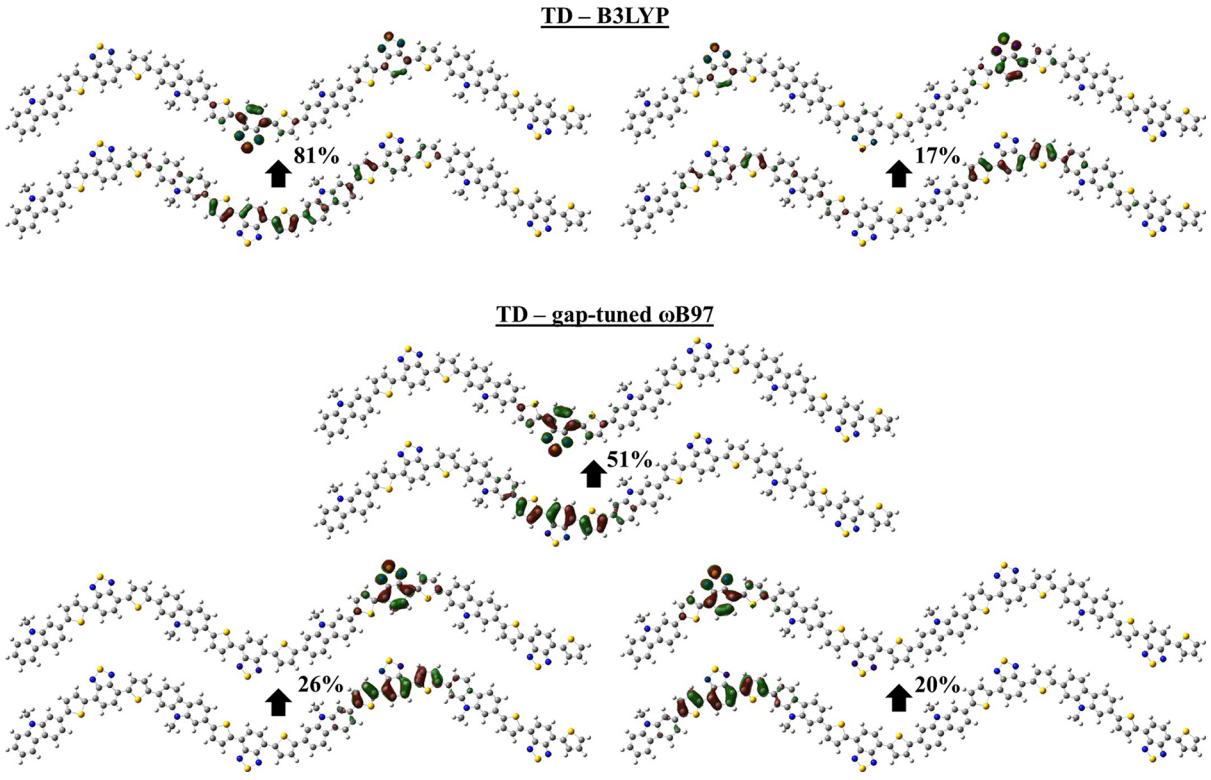

Figure 9. TD-DFT natural transition orbitals for the S_0−S_1 transition in the tetramer of the low-band-gap polymer PCDTBT (poly[*N*-alkyl-2,7-carbazole-*alt*-5,5-(40,70-di-2-thienyl-20,10,30-benzothiadiazole)]) determined from B3LYP and gap-tuned ωB97.[38] The numbers specify the weight of the respective particle-hole contributions. The electron−hole pairs predicted from the tuned LRC-hybrid are much more localized than those predicted by standard functionals such as B3LYP.

dx.doi.org/10.1021/ar500021t | *Acc. Chem. Res.* 2014, 47, 3284−3291

EXCITED STATE PROPERTIES

Low-Band-Gap Polymers

Due to their potential for harnessing an important part of the solar spectrum, polymers with a low optical gap are frequently used materials in organic solar cells. Typically, a low-lying optical transition is obtained by combining electron-rich and electron-deficient fragments along the polymer backbone, leading to excited states with a significant charge-transfer (CT) character. While standard hybrid functionals are well-known to underestimate the energies of such CT-type excitation energies significantly, LRC-hybrid functionals with a tuned range-separation parameter ω have been reported to yield improved excitation energies for CT-type excitations.[37] This is achieved by tuning ω to a criterion that not only includes the IP but also the electron affinity (EA) of the system of interest. This procedure is referred to as gap-tuning.[24,25,37] Typically, gap-tuning leads to ω-values close to the IP-tuned ones with a similar dependency on conjugation and system size.[24,25,38]

Indeed, the gap-tuning procedure leads to a significant improvement in the calculated optical absorption spectrum of low-band-gap polymers as compared to standard global and LRC hybrid functionals.[38] In addition, the tuned LRC-hybrid functionals also change the nature of the excited states. This is highlighted in Figure 9, which depicts the natural transition orbitals for the S_0-S_1 transition in the tetramer of the low-band-gap polymer PCDTBT determined from B3LYP and gap-tuned ωB97. While B3LYP predicts the electron−hole pairs corresponding to the S_0-S_1 transition to be delocalized over several donor and acceptor moieties, the gap-tuned ωB97 calculations suggests a qualitatively different picture. Here, the electron−hole pairs are much more localized, while strongly coupled to one another.[38] This clearly demonstrates that the delocalization error inherent to global hybrid functionals such as B3LYP also has important consequences for the description of excited states. The good agreement of the gap-tuned ωB97 spectrum with experiment suggests that the reduced delocalization error in tuned LRC-hybrid functionals is of great value also for the description of excited state properties of organic electronic materials.[38] It is also useful to note that the tuning procedure has been found to reduce the occurrence of triplet instabilities and leads to an overall significantly improved prediction of triplet excitation energies when using LRC-hybrid functionals in TD-DFT.[39]

CONCLUDING REMARKS

In this Account, we have illustrated that the spurious localization/delocalization errors inherent to HF and standard DFT functionals can lead to significant qualitative and quantitative failures in the evaluation of the ground- and excited-state properties of organic electronic materials. In particular, the widely employed semilocal and global hybrid functionals tend to overestimate the delocalization of electron and hole densities. In contrast, LRC hybrid functionals with standard range-separation parameters tend to overlocalize electron densities in π-conjugated chains, leading to an underestimation of torsional barriers and triplet energies and an overestimation of the bond-length alternation in polyenes.

These errors can be reduced significantly by nonempirically tuning the range-separation parameter ω in LRC hybrid functionals to fulfill the IP theorem. Using this system-specific ω, many of the problems related to a spurious (de)localization of electrons can be solved. This includes the determination of geometry and electronic couplings in organic mixed-valence systems as well as torsional barriers, charge-transfer excitations, and triplet instabilities in long π-conjugated molecular chains. Looking forward, we anticipate that future developments in this field will need to tackle the most prominent drawback of the tuned LRC hybrid functionals, that is, their lack of size consistency. Avenues to do so may involve range-separation of the correlation hole or using a local, density-dependent range-separation.

AUTHOR INFORMATION

Corresponding Authors

*Email: jean-luc.bredas@chemistry.gatech.edu.
*E-mail: koerz@uni-potsdam.de.

Present Address

[§]J.-L.B., as of July 2014: Division of Physical Sciences and Engineering, King Abdullah University of Science and Technology, Thuwal 23955-6900, Kingdom of Saudi Arabia (e-mail: jean-luc.bredas@kaust.edu.sa).

Notes

The authors declare no competing financial interest.

Biographies

Thomas Körzdörfer is a Junior Professor for Computational Chemistry at the Institute of Chemistry of the University of Potsdam, Germany. Prior to joining the faculty at the University of Potsdam in the summer of 2012, he stayed as a postdoctoral researcher at the Georgia Institute of Technology where he worked with Jean-Luc Brédas. He received a diploma in physics (2006), a diploma supplement in macromolecular science (2008), and a Dr. rer. nat. in theoretical physics (2009) from the University of Bayreuth. His group at the University of Potsdam works on the development of electronic-structure methods for the description of organic electronic materials.

Jean-Luc Brédas is currently Regents' Professor of Chemistry and Biochemistry and holds the Vasser-Woolley and Georgia Research Alliance Chair in Molecular Design at the Georgia Institute of Technology. In July 2014, he will join the King Abdullah University of Science and Technology in Thuwal, Saudi Arabia, as Distinguished Professor of Materials Science and Engineering and the Rawabi Holding Research Chair in Solar Energy Science and Engineering. His research interests focus on the theoretical understanding and design of novel organic materials for electronic and photonic applications.

ACKNOWLEDGMENTS

We thank R. Parrish and D. Sherrill for the implementation of fractional-particle DFT, as well as J. Sears, C. Sutton, L. Pandey, V. Coropceanu, and C. Risko for helpful and stimulating discussions. This work has been supported by the National Science Foundation under its CRIF Program and by the Office of Naval Research.

REFERENCES

(1) Shirakawa, H.; Louis, E. J.; MacDiarmid, A. G.; Chiang, C. K.; Heeger, A. J. Synthesis of electrically conducting organic polymers: halogen derivatives of polyacetylene, (CH). *J. Chem. Soc., Chem. Commun.* **1977**, 578−580.
(2) Hohenberg, P.; Kohn, W. Inhomogeneous Electron Gas. *Phys. Rev.* **1964**, *136*, B864−B871.
(3) Sham, L. J.; Kohn, W. One-Particle Properties of an Inhomogeneous Interacting Electron Gas. *Phys. Rev.* **1966**, *145*, 561−567.

(4) Runge, E.; Gross, E. K. U. Density-Functional Theory for Time-Dependent Systems. *Phys. Rev. Lett.* **1984**, *52*, 997−1000.
(5) Perdew, J. P.; Burke, K.; Ernzerhof, M. Generalized Gradient Approximation Made Simple. *Phys. Rev. Lett.* **1996**, *77*, 3865−3868; *Erratum: Phys. Rev. Lett.* **1997**, *78*, 1396.
(6) Zhao, Y.; Truhlar, D. G. A new local density functional for main-group thermochemistry, transition metal bonding, thermochemical kinetics, and noncovalent interactions. *J. Chem. Phys.* **2006**, *125*, 194101.
(7) Stephens, P. J.; Devlin, F. J.; Chabalowski, C. F.; Frisch, M. J. Ab Initio Calculation of Vibrational Absorption and Circular Dichroism Spectra Using Density Functional Force Fields. *J. Phys. Chem.* **1994**, *98*, 11623−11627.
(8) Adamo, C.; Barone, V. Toward reliable density functional methods without adjustable parameters: The PBE0 model. *J. Chem. Phys.* **1999**, *110*, 6158−6170.
(9) Zhao, Y.; Truhlar, D. The M06 suite of density functionals for main group thermochemistry, thermochemical kinetics, noncovalent interactions, excited states, and transition elements: two new functionals and systematic testing of four M06-class functionals and 12 other functionals. *Theor. Chem. Acc.* **2008**, *120*, 215−241.
(10) Ruzsinszky, A.; Perdew, J. P.; Csonka, G. I.; Vydrov, O. A.; Scuseria, G. E. Spurious fractional charge on dissociated atoms: Pervasive and resilient self-interaction error of common density functionals. *J. Chem. Phys.* **2006**, *125*, 194112.
(11) Mori-Sánchez, P.; Cohen, A. J.; Yang, W. Many-electron self-interaction error in approximate density functionals. *J. Chem. Phys.* **2006**, *125*, 201102.
(12) An aug-cc-pVTZ basis set was used for the FCI and CCSD calculations.
(13) Perdew, J. P.; Zunger, A. Self-interaction correction to density-functional approximations for many-electron systems. *Phys. Rev. B* **1981**, *23*, 5048−5079.
(14) Cohen, A. J.; Mori-Sanchez, P.; Yang, W. Insights into Current Limitations of Density Functional Theory. *Science* **2008**, *321*, 792−794.
(15) Perdew, J. P.; Parr, R. G.; Levy, M.; Balduz, J. L., Jr. Density-Functional Theory for Fractional Particle Number: Derivative Discontinuities of the Energy. *Phys. Rev. Lett.* **1982**, *49*, 1691−1694.
(16) Kümmel, S.; Kronik, L. Orbital-dependent density functionals: Theory and applications. *Rev. Mod. Phys.* **2008**, *80*, 3−60.
(17) Cohen, A. J.; Mori-Sanchez, P.; Yang, W. Challenges for Density Functional Theory. *Chem. Rev.* **2011**, *112*, 289−320.
(18) Baer, R.; Livshits, E.; Salzner, U. Tuned Range-Separated Hybrids in Density Functional Theory. *Annu. Rev. Phys. Chem.* **2010**, *61*, 85−109.
(19) Körzdörfer, T.; Parrish, R. M.; Marom, N.; Sears, J. S.; Sherrill, C. D.; Brédas, J.-L. Assessment of the performance of tuned range-separated hybrid density functionals in predicting accurate quasiparticle spectra. *Phys. Rev. B* **2012**, *86*, 205110.
(20) Savin, A.; Flad, H.-J. Density functionals for the Yukawa electron-electron interaction. *Int. J. Quantum Chem.* **1995**, *56*, 327−332.
(21) Vydrov, O. A.; Scuseria, G. E. Assessment of a long-range corrected hybrid functional. *J. Chem. Phys.* **2006**, *125*, 234109.
(22) Chai, J. D.; Head-Gordon, M. Systematic optimization of long-range corrected hybrid density functionals. *J. Chem. Phys.* **2008**, *128*, 084106.
(23) Stein, T.; Kronik, L.; Baer, R. Reliable Prediction of Charge Transfer Excitations in Molecular Complexes Using Time-Dependent Density Functional Theory. *J. Am. Chem. Soc.* **2009**, *131*, 2818−2820.
(24) Refaely-Abramson, S.; Baer, R.; Kronik, L. Fundamental and excitation gaps in molecules of relevance for organic photovoltaics from an optimally tuned range-separated hybrid functional. *Phys. Rev. B* **2011**, *84*, 075144.
(25) Stein, T.; Eisenberg, H.; Kronik, L.; Baer, R. Fundamental Gaps in Finite Systems from Eigenvalues of a Generalized Kohn-Sham Method. *Phys. Rev. Lett.* **2010**, *105*, 266802.
(26) Refaely-Abramson, S.; Sharifzadeh, S.; Govind, N.; Autschbach, J.; Neaton, J. B.; Baer, R.; Kronik, L. Quasiparticle Spectra from a Nonempirical Optimally Tuned Range-Separated Hybrid Density Functional. *Phys. Rev. Lett.* **2012**, *109*, 226405.
(27) Körzdörfer, T.; Sears, J. S.; Sutton, C.; Brédas, J.-L. Long-range corrected hybrid functionals for pi-conjugated systems: Dependence of the range-separation parameter on conjugation length. *J. Chem. Phys.* **2011**, *135*, 204107.
(28) Robin, M. B.; Day, P. Mixed Valence Chemistry - A Survey and Classification. In *Advances in Inorganic Chemistry and Radiochemistry*; Emeleus, H. J., Sharpe, A. G., Eds.; Academic Press: Waltham, MA, 1967; Vol. *10*; pp 247−422.
(29) Sutton, C.; Körzdörfer, T.; Coropceanu, V.; Brédas, J.-L. Toward a Robust Quantum-Chemical Description of Organic Mixed-Valence Systems. *J. Phys. Chem. C* **2013**, *118*, 3925−3934.
(30) Glaesemann, K. R.; Govind, N.; Krishnamoorthy, S.; Kowalski, K. EOMCC, MRPT, and TDDFT Studies of Charge Transfer Processes in Mixed-Valence Compounds: Application to the Spiro Molecule. *J. Phys. Chem. A* **2010**, *114*, 8764−8771.
(31) Sears, J. S.; Chance, R. R.; Brédas, J. L. Torsion Potential in Polydiacetylene: Accurate Computations on Oligomers Extrapolated to the Polymer Limit. *J. Am. Chem. Soc.* **2010**, *132*, 13313−13319.
(32) Sutton, C.; Körzdörfer, T.; Gray, M. T.; Brunsfeld, M.; Parrish, R. M.; Sherrill, C. D.; Sears, J. S.; Brédas, J.-L. Accurate description of torsion potentials in conjugated polymers using density functionals free of self-interaction error. *J. Chem. Phys.* **2014**, *140*, 054310.
(33) Meier, H.; Stalmach, U.; Kolshorn, H. Effective conjugation length and UV/vis spectra of oligomers. *Acta Polym.* **1997**, *48*, 379−384.
(34) Körzdörfer, T.; Parrish, R. M.; Sears, J. S.; Sherrill, C. D.; Brédas, J.-L. On the relationship between bond-length alternation and many-electron self-interaction error. *J. Chem. Phys.* **2012**, *137*, 124305.
(35) Yannoni, C. S.; Clarke, T. C. Molecular Geometry of cis- and trans-Polyacetylene by Nutation NMR Spectroscopy. *Phys. Rev. Lett.* **1983**, *51*, 1191−1193.
(36) Karolewski, A.; Kronik, L.; Kümmel, S. Using optimally tuned range separated hybrid functionals in ground-state calculations: Consequences and caveats. *J. Chem. Phys.* **2013**, *138*, 204115.
(37) Kuritz, N.; Stein, T.; Baer, R.; Kronik, L. Charge-Transfer-like $\pi-\pi^*$ Excitations in Time-Dependent Density Functional Theory: A Conundrum and Its Solution. *J. Chem. Theory Comput.* **2011**, *7*, 2408−2415.
(38) Pandey, L.; Doiron, C.; Sears, J. S.; Bredas, J.-L. Lowest excited states and optical absorption spectra of donor-acceptor copolymers for organic photovoltaics: a new picture emerging from tuned long-range corrected density functionals. *Phys. Chem. Chem. Phys.* **2012**, *14*, 14243−14248.
(39) Sears, J. S.; Körzdörfer, T.; Zhang, C.-R.; Brédas, J.-L. Communication: Orbital instabilities and triplet states from time-dependent density functional theory and long-range corrected functionals. *J. Chem. Phys.* **2011**, *135*, 151103.